Protonium formation in antiproton–hydrogen-atom collisions

S. Yu. Ovchinnikov* and J. H. Macek
Department of Physics and Astronomy, University of Tennessee, Knoxville, Tennessee 37996-1200, USA
and Oak Ridge National Laboratory, Oak Ridge, Tennessee 37831, USA
(Received 10 November 2004; published 31 May 2005)

Expressions for momentum distributions of electrons in antiproton–hydrogen-atom collisions are derived in the framework of the advanced adiabatic approach for the time- independent Schrödinger equation. Protonium formation cross sections for states with different n and l spherical quantum numbers are also obtained. Total ionization and protonium formation cross sections are compared with other calculations in the interval of impact energies from 0.5 eV to 10 keV. We show that diabatic states promoted into the continuum can be rigorously defined within the advanced adiabatic framework.

DOI: 10.1103/PhysRevA.71.052717 PACS number(s): 34.50.Fa

I. INTRODUCTION

Cross sections for protonium formation are important for designing antiproton traps since trapped antiprotons undergo atomic reactions with background gases which remove them from the trap. First, antiprotons are captured into highly excited bound states by ejecting the bound electrons, then they are radiationally deexcited, and, finally, they annihilate by nuclear interactions. An understanding of these process requires reliable cross sections for low-energy collisions of antiprotons with atoms.

This article presents expressions for energy and angular distributions of electrons in antiproton–hydrogen-atom collisions in terms of the finite-dipole eigenfunctions and eigenvalues calculated for complex dipole moments. The expressions were derived in the framework of the advanced adiabatic approach [1]. We test them in the interval of impact energies from 0.5 eV to 10 keV by integrating electron spectra over momentum and comparing the total ionization and protonium formation cross sections with other calculations [2–7]. Using conservation of total energy and angular momentum below the ionization threshold we obtain protonium formation cross sections for states with different n and l spherical quantum numbers.

At present, ionization cross sections based on semiclassical methods [2,5] that are essentially exact for energies above a few hundred eV for projectiles whose masses are comparable to the proton mass have been reported. In this energy range protonium formation cross sections are extremely small and a wide variety of techniques can be reliably employed to compute ionization cross sections. Important for designing antiproton traps, however, are energies in the $0-50$ eV range. The hyperspherical representation is readily adapted to this region; however, hyperspherical adiabatic methods are impractical owing to the need for large numbers of basis states that are difficult to compute [8]. In this energy range a wave treatment for the relative motion of the nuclei [5] is needed since the $p\bar{p}$ system is bound in the final state and protonium in specific n,l states are not represented in standard adiabatic bases. For these reasons, the n and l distributions that are available at the present time employ the Born approximation [9], the continuous-time Monte Carlo (CTMC) method [4], the FMD method [10], or the diabatic-state method [11]. A version of CTMC that employs model potentials incorporating quantum corrections [12] is referred to as the KW or FMD method [10]. Comprehensive discussion of these calculations and calculations for negative exotic particles other than antiprotons can be found in the review article of Cohen [13].

A theory developed by Solov'ev [1] and known as the advanced adiabatic theory circumvents many problems that hinder quantum computations of ionization at low impact energies. The advanced adiabatic theory is based on the time-energy Fourier transformation. This transformation takes into account the time delay of the outgoing wave packet related to the ionization and associated with the Hamiltonian at the moment of ionization. Therefore the advanced adiabatic theory employs the function $t(\varepsilon)$ inverse to the adiabatic energy $\varepsilon(t)$ and applies to any system where there is an adiabatic parameter that varies with time t. It has been successfully used to compute ionization energy and angular distributions in ion-atom collisions.

The key idea of this theory is to obtain formulas that are exact in the limit as the *initial* impact velocity vanishes, i.e., as $v \to 0$. Of course, the limit $v \to 0$ is a mathematical limit on a computed amplitude and does not suppose that the limit can actually be taken experimentally. Even so, it is reasonable to suppose that a result that is exact in the limit $v \to 0$ will be reliable for $v \ll \langle v_e \rangle$ where $\langle v \rangle$ is the mean electron velocity in the initial or final states. In the processes considered here $v \approx 1/6$ and $\langle v_e \rangle \approx 1$ so that the inequality is well satisfied.

A limitation of this now standard advanced adiabatic approximation is the use of a common classical trajectory for relative motion of heavy particles. This is not a conceptual limitation and can be readily relaxed as done by Demkov and Osherov [14] in their discussion of exact solutions for the multicrossing model, a precursor of the advanced adiabatic theory. It is similarly shown in this manuscript how the advanced adiabatic theory is readily adapted to the time-independent Schödinger equation. The wave version employs the function $R(\varepsilon)$ inverse to the adiabatic energy $\varepsilon(R)$

*Also at A. F. Ioffe Physico-Technical Institute, St. Petersburg 194021, Russia. Electronic address: serge@charcoal.phys.utk.edu

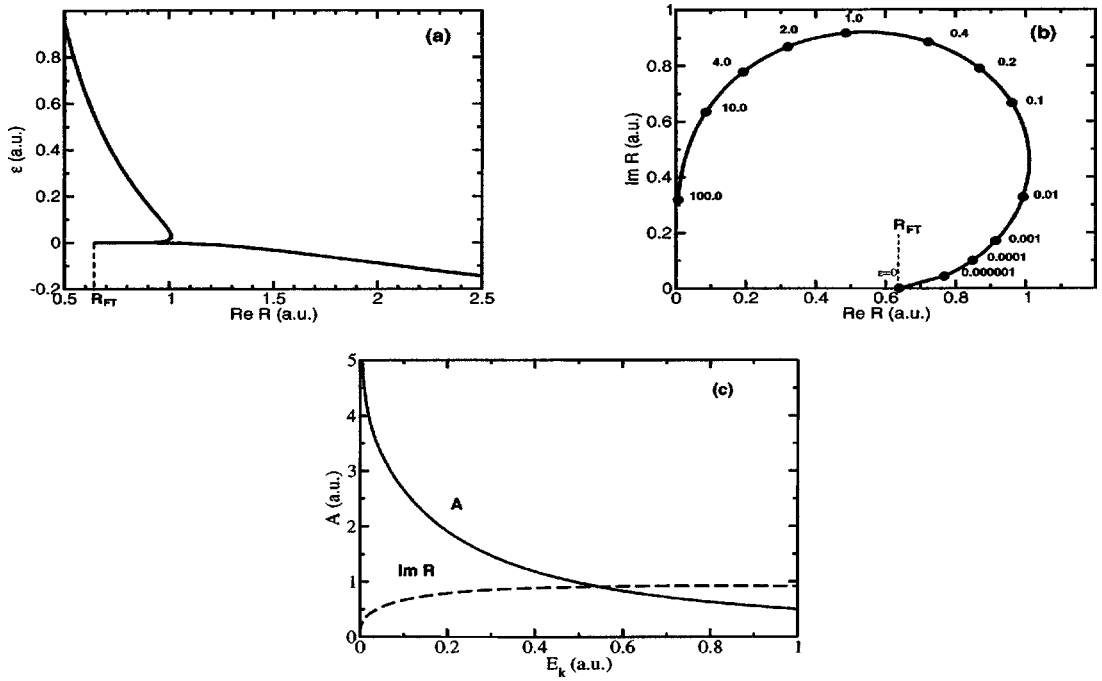

FIG. 1. (a) The lowest adiabatic potential curve $\varepsilon(R)<0$ of the finite dipole as a function of the internuclear separation R joined at the Fermi-Teller radius $R=R_{\mathrm{FT}}$ to the real argument ε of the complex function $R(\varepsilon)$ for $\varepsilon>0$. (b) Parametric plot of Re R and Im R as a function of the real variable ε for the quasistationary state continued from the lowest bound state. (c) Coefficient $A(\varepsilon)$ used in Eq. (1).

where the internuclear distance R in place of t. The present article reports calculations of ionization and protonium formation including n and l distributions of the protonium states using this wave version of the advanced adiabatic theory. The resulting wave version of the advanced adiabatic theory is used to compute energy and angular distributions of electrons for low-energy impact of antiprotons on atomic hydrogen.

II. ADVANCED ADIABATIC THEORY

The conventional adiabatic electron energies for an electron in the field of $p+\bar{p}$ are known as the potential curves of the finite dipole. In the separated-atom limit they are the Stark energy levels of the H atom in the field of the antiproton. At the united-atom limit, where the antiproton coincides with the proton, the electron nuclei potentials cancel and the electron is completely free. At some finite distance, called the Fermi-Teller radius $R_{\mathrm{FT}}=0.6393\ldots$ the electron just becomes unbound in the finite dipole field of the $p\bar{p}$ system. The lowest adiabatic potential curve of the finite dipole is shown in Fig. 1(a) below $\varepsilon=0$. Since the point $R=R_{\mathrm{FT}}$ is an essential singularity [15], adiabatic functions $\varepsilon(R)$ have no limits at this point. Therefore dynamics are difficult to describe using adiabatic states.

In the advanced adiabatic theory the energy distribution of emitted electrons integrated over the electron directions is given by the probability $P(\varepsilon_{\boldsymbol{k}})$, namely, Eq. (16) of Ref. [1],

$$P(\varepsilon_{\boldsymbol{k}}) = A(\varepsilon_{\boldsymbol{k}}) \left| \frac{dt}{dR} \exp\left(i2 \int_{\varepsilon_i}^{\varepsilon_{\boldsymbol{k}}} t(\varepsilon) d\varepsilon \right) \right|, \tag{1}$$

where

$$A(\varepsilon) = \sqrt{2\varepsilon} \left| \frac{dR(\varepsilon)}{d\varepsilon} \right| \int |C(\varepsilon;\hat{\boldsymbol{r}})|^2 d\hat{\boldsymbol{r}}, \tag{2}$$

ε_i is the electronic energy of the initial state, $\varepsilon_{\boldsymbol{k}}$ is the energy of the ionized electron, and $C(\varepsilon;\hat{\boldsymbol{r}})$ is the coefficient of the outgoing electron wave $\exp(i\sqrt{2\varepsilon}r)/r$ of the finite dipole wave function $\Phi(\varepsilon;\boldsymbol{r})$, which satisfies the Schödinger equation for the finite dipole

$$\left[-\frac{1}{2}\nabla_{\boldsymbol{r}}^2 + \frac{1}{|\boldsymbol{r}+[R(\varepsilon)/2]\hat{\boldsymbol{z}}|} - \frac{1}{|\boldsymbol{r}-[R(\varepsilon)/2]\hat{\boldsymbol{z}}|} \right] \Phi(\varepsilon;\boldsymbol{r}) = \varepsilon \Phi(\varepsilon;\boldsymbol{r}), \tag{3}$$

with boundary conditions

$$|\Phi(\varepsilon;0)| < \text{const},$$

$$\Phi(\varepsilon;\boldsymbol{r}) \to \frac{C(\varepsilon;\hat{\boldsymbol{r}})}{r} \exp(i\sqrt{2\varepsilon}r) \quad \text{as } r \to \infty. \tag{4}$$

The wave function $\Phi(\varepsilon;\boldsymbol{r})$ is normalized according to

$$\int \Phi^2(\varepsilon;\boldsymbol{r}) d^3\boldsymbol{r} = 1. \tag{5}$$

Calculations of $R(\varepsilon)$, $C(\varepsilon;\hat{\boldsymbol{r}})$, and $A(\boldsymbol{\varepsilon})$ are based on the separation of the variables in spheroidal coordinates and are carried out using the algorithm discussed in Ref. [16]. Figure 1(b) shows the computed $R(\varepsilon)$ in the form of a parametric plot. The function Re $R(\varepsilon)$ can be easily inverted to obtain the multivalued function $\varepsilon(\mathrm{Re}\,R)$ shown in Fig. 1(a). A diabatic single-valued function $\varepsilon_D(R)$ can be constructed by smoothing the spike near $\varepsilon=0$. Such a diabatic energy has no

TABLE I. Advanced adiabatic functions for positive energy.

$\varepsilon_{\boldsymbol{k}}$ (a.u.)	Re R (a.u.)	Im R (a.u.)	$\lvert A\rvert$ (a.u.)
0	0.6393	0	0
0.00001	0.8009	0.0636	11.02
0.00002	0.8133	0.0722	15.04
0.00004	0.8318	0.0863	15.66
0.0001	0.8477	0.0996	15.34
0.0002	0.8654	0.1158	13.16
0.0004	0.8849	0.1358	9.548
0.001	0.9138	0.1703	6.675
0.002	0.9374	0.2046	5.725
0.004	0.9620	0.2484	5.072
0.01	0.9921	0.3267	4.443
0.02	1.0076	0.4060	3.984
0.04	0.9620	0.5423	3.441
0.1	0.9598	0.6656	2.614
0.2	0.8676	0.7897	1.921
0.4	0.7220	0.8842	1.151
1	0.4868	0.9167	0.4797
2	0.3203	0.8675	0.2341
4	0.1925	0.7774	0.09772
10	0.08577	0.6345	0.03117

imaginary part and the state is promoted to the continuum at $R=R_D\approx 1$ a.u. Note that the spike for $R<R_D$ seen in Fig. 1(a) implies that fixed-nucleus bound dipole states do not realistically describe the electrons in the dipole fields of two heavy particles when $R<R_D$. In essence, dipole states do not actually exist for $R<R_D$. Numerical values of the function $A(\varepsilon)$ computed for the finite dipole case are shown in Fig. 1(c) and tabulated in Table I.

In the advanced adiabatic framework the dynamics are related to $\mathrm{Im}\,R(\varepsilon)$, shown in Fig. 1(c), rather than $\Gamma=2\,\mathrm{Im}\,\varepsilon(R)$ used in survival probability calculations. The survival probability technique gives reliable results, that agree with the advanced adiabatic results, only when $\Gamma(R)\ll\mathrm{Re}\,\varepsilon(R)$ [1], since it does not take into account the time delay due to propagation of the outgoing wave packet of emitted electrons. In the case of the finite dipole [17] $\Gamma(R)\gg|\mathrm{Re}\,\varepsilon(R)|$ and $\varepsilon(R)$ is discontinuous at $R=R_{\mathrm{FT}}$, since $R=R_{\mathrm{FT}}$ is an essential singularity.

III. CROSS SECTIONS FOR IONIZATION AND PROTONIUM FORMATION

To transform Eq. (1) from the time-dependent to the time-independent representation the time is replaced by the generalized time parameter

$$t=-\frac{\partial S}{\partial E}, \tag{6}$$

where S is the classical action and E is the total energy, which equals the collision energy in the center-of-mass frame of reference. The classical action is the sum of the classical actions in the initial and final states

$$S=\int_{R_i}^{R_M}K(R)dR+\int_{R_M}^{R_T}K_f(R)dR, \tag{7}$$

where

$$K(R)=\sqrt{2\mu[E-\varepsilon(R)-(L+1/2)^2/2\mu R^2+1/R]},$$

$$K_f(R)=\sqrt{2\mu[E-\varepsilon_{\boldsymbol{k}}-(L+1/2)^2/2\mu R^2+1/R]}, \tag{8}$$

and where μ is the reduced mass of colliding particles, L is the total angular momentum, R_i is a large value of R on the initial branch of $\varepsilon(R)$, R_T is the turning point in final channel, and R_M is the complex value of R where $\varepsilon(R)=\varepsilon_{\boldsymbol{k}}$. The matching radii R_M as function of $\varepsilon_{\boldsymbol{k}}$ are shown on Fig. 1(b).

The time replacement of Eq. (6), when substituted into Eq. (1), gives the energy and angular distributions of emitted electrons in the form

$$P(\varepsilon_{\boldsymbol{k}})=A(\varepsilon_{\boldsymbol{k}})\left|\frac{dK(R_M)}{dE}\exp(i2S)\right|. \tag{9}$$

The integral for the classical action in the initial state Eq. (7) goes along the real axis from R_i to R_{FT} and along the contour in Fig. 1(b), from R_{FT} to R_M. The integral for the classical action in the final state is evaluated analytically.

Equation (9) is the principal result of the work reported here. It gives an essentially closed-form expression for the ionization cross section for electrons ejected from atomic hydrogen in terms of two functions, namely, $R(\varepsilon)$, or equivalently $\varepsilon(R)$ and $A(\varepsilon)$ obtained by solving the finite dipole Schrödinger equation Eq. (3). These quantities are tabulated in Tables I and II on a grid of energies sufficient for numerical evaluation of S in Eq. (7). This gives an effectively closed-form result that can be used to find ionization probabilities for any desired value of the parameters, namely, the ejected electron energy $\varepsilon_{\boldsymbol{k}}$, the total energy E, and the total orbital angular momentum L. Below, we show how this same expression is used to compute protonium formation.

For calculations of ionization when $E>0$ it is useful to note that the first integral in Eq. (7) includes the part from R_i to R_{FT} involving $\varepsilon(R)$ tabulated in Table II. This part of the action is real and contributes a phase to the S-matrix element so it can be omitted. Only the integral from R_{FT} to R_M contributes to the imaginary part of the action.

This latter integral is best done by changing integration variables to ε. We then use a simple numerical integration technique that gives

$$\int_{R_{\mathrm{FT}}}^{R_M}K(R)dR\approx\frac{1}{2}\sum_{k=0}^{N}[K(R(\varepsilon_k))+K(R(\varepsilon_{k+1}))]\times[R(\varepsilon_{n+1})-R(\varepsilon_k)] \tag{10}$$

where

$$K(R(\varepsilon_k))=\sqrt{2M\left[E-\varepsilon_k-\frac{(L+1/2)^2}{2\mu R^2(\varepsilon_k)}+\frac{1}{R(\varepsilon_k)}\right]}. \tag{11}$$

TABLE II. Lowest adiabatic potential curve.

R (a.u.)	$\varepsilon(R)$ (a.u.)
2.5	−0.143582
2.4	−0.133133
2.3	−0.122326
2.2	−0.111189
2.1	−0.0997689
2	−0.0881331
1.9	−0.0763773
1.8	−0.0646324
1.7	−0.0530728
1.6	−0.041924
1.5	−0.0314673
1.4	−0.0220371
1.3	−0.0140013
1.2	−0.00771014
1.1	−0.0033967
1	−0.00102467
0.9	−0.000148709
0.8	−3.64512e−06
0.78	−1.07992e−06
0.76	−2.36022e−07
0.74	−3.29193e−08
0.72	−2.25025e−09

When $E<0$, electrons can still be ejected with positive energy $\varepsilon_{\boldsymbol{k}}$, but now the system must tunnel from R_i to R_{FT}. In this case the integral from R_i to R_{FT} contributes to the imaginary part of the action and cannot be omitted. Of course, since $E<0$, the antiproton and proton must be bound. The procedure to calculate this process is discussed below.

If the quantity $E-\varepsilon_{\boldsymbol{k}}$ is negative, then there are two turning points in the final channel and the wave function is bounded as $R\to\infty$ only when the integral between the two turning points takes on half integral multiples of π, i.e., the R motion is quantized according to

$$E-\varepsilon_{\boldsymbol{k}}=-\frac{1}{2}\frac{\mu}{n^2}, \tag{12}$$

where $-\mu/(2n^2)$ is the binding energy of the nth state of protonium. Therefore the ionization amplitude becomes the amplitude for the rearrangement process

$$\bar{p}+H\to(\bar{p},p)_n+e^- \tag{13}$$

up to a normalization constant. In this way one extracts the rearrangement amplitude even though no protonium states are included in the basis set.

There is little difference theoretically between ionization with and without protonium formation as is apparent from the continuity of ionization cross sections across the protonium threshold seen in CTMC calculations [2,4]. This allows a simple way to compute protonium formation in the advanced adiabatic theory, namely, we compute ionization

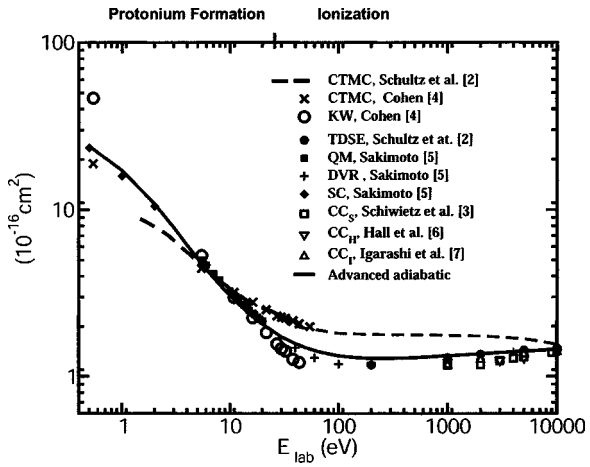

FIG. 2. Cross sections for ionization and protonium formation, where $E_{\mathrm{lab}}=2E$.

without reference to the quantization of the protonium energies and then identify the cross section for negative values of $E-\varepsilon_{\boldsymbol{k}}$ with protonium formation. This is convenient for computations of total protonium formation cross sections. Using the standard [11] $d\varepsilon_{\boldsymbol{k}}/dn$ energy interval weighting one obtains the n, l distributions of the protonium in the form

$$f_{n,l}=\frac{\mu}{n^3}P\left(E+\frac{1}{2}\frac{\mu}{n^2}\right) \tag{14}$$

and the angular momentum l of the protonium state is $l\approx L$, since the emitted electron has a small angular momentum.

We compute total ionization and protonium formation cross sections for low-energy impact of antiprotons on atomic hydrogen by integrating electron spectra Eq. (9) over $\varepsilon_{\boldsymbol{k}}$. The results of our calculations are shown in Fig. 2 for energies between 0.5 eV and 10 keV. In the energy range 200 eV$<E<$10 keV, where the protonium formation cross sections are negligible, the advanced adiabatic results are in good agreement with essentially exact solutions of the time-dependent Schrödinger equation in the straight line approximation by Schultz *et al.* using a lattice technique [2] (TDSE), Sakimoto using a discrete-variable representation (DVR) method [5], and atomic coupled-channel calculations of Schiwietz *et al.* [3] (CC_S), of Hall *et al.* [6] (CC_H), and of Igarashi *et al.* [7] (CC_I).

Below the ionization threshold at $E_{\mathrm{lab}}=2E=27.2$ eV, electron ejection is uniquely associated with protonium formation. In this region the advanced adiabatic theory is most reliable since the relative velocities of the heavy particles become much smaller than the electron velocities. Figure 2 shows good agreement between our advanced adiabatic calculations of total protonium formation cross sections and full quantum-mechanical (QM) and semiclassical (SC) calculations of Sakimoto [5]. The present results fall in between the KW-FMD and CTMC results at low energy.

At very low energies, antiprotons may be temporarily trapped in the combined polarization and centrifugal potentials $V_{\mathrm{eff}}=L(L+1)/2\mu R^2-\alpha_p/2R^4$, where $\alpha_p=9/2$ is the polarizability of the hydrogen atom. The associated orbiting

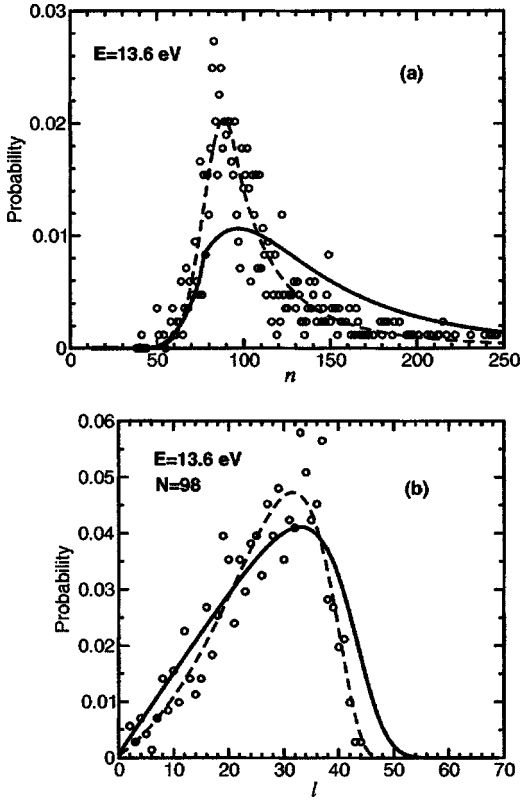

FIG. 3. (a) Probabilities for protonium formation as a function of n for the initial energy $E=13.6$ eV. Solid curve, this work; circles, KW-FMD, Ref. [4]; dashed curve, the recommended fit, Ref. [4]. (b) Probabilities for protonium formation in the selective l states for $n=98$.

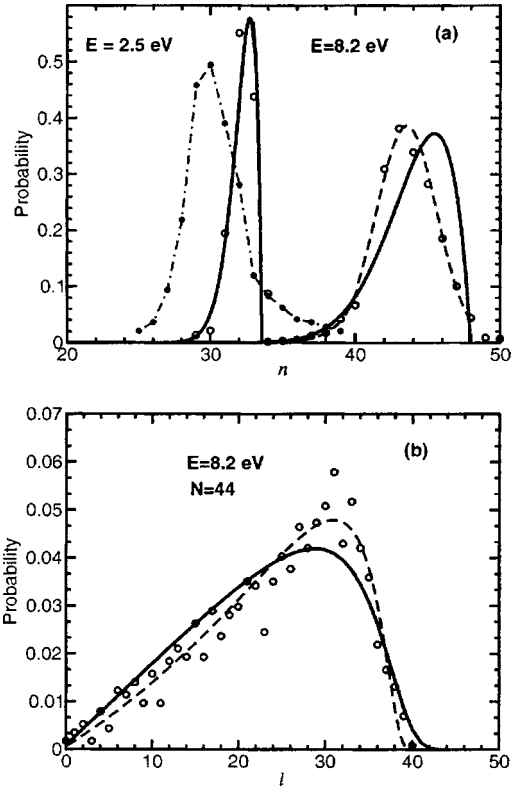

FIG. 4. (a) Probabilities for protonium formation as a function of n for the initial energy $E=8.2$ and 2.5 eV. Solid curve, this work; circles, KW-FMD, Ref. [4]; dashed curve, the recommended fit, Ref. [4]; dot-dashed curve, Ref. [18]. (b) Probabilities for protonium formation in the selective l states for $n=44$.

resonances can decay by electron emission thereby leading to protonium formation via a process similar to associative ionization in negative ion collisions. If one assumes unit probability for decay via electron emission then one obtains the Langevin cross section (sometime called the orbiting cross section) σ_p [5] for protonium formation given by $\sigma_p = 2\pi\sqrt{\alpha_p/E}$, an estimate that is thought to be exact for vanishingly small E. According to Sakimoto [5] the orbiting cross sections match semiclassical calculations [5] and therefore our calculations for $E<0.3$ eV.

IV. PROBABILITIES FOR PROTONIUM FORMATION IN THE SELECTIVE *n* AND *l* STATES

Using conservation of total energy and total angular momentum we compute distributions of protonium formation cross sections over states with different n and l spherical quantum numbers. Results of our calculations of these distributions are shown in Figs. 3(a) and 3(b) for $E=13.6$ eV and in Figs. 4(a) and 4(b) for $E=8.2$ eV. The n distributions are similar to KW calculations of Cohen [4] in all cases, although Fig. 2 indicates that the KW-FMD total cross sections are a factor of 2 larger than the advanced adiabatic at 0.5 eV. A possible explanation of this discrepancy and how to improve the KW-FMD calculations are discussed in the review article [13].

Our results and those of Ref. [4], maximize at $n=32$ or 33. A more elaborate survival probability calculation was recently published [18] for $E=2.5$ eV. Their n distribution shown in Fig. 4 maximizes at $n=30$ and has a tail extending to $n=39$, but, by energy conservation, the highest n that could be populated is $n=33$. The high-n tail indicates a limitation of the approximate calculations of Ref. [18].

V. SUMMARY

The most notable feature of the l distributions is their nonstatistical nature with a rapid decrease at a value l significantly less than the maximum. This decrease occurs when the classical turning radius R_T exceeds R_D so that the amplitude of the final-state wave function is small for $R \approx R_D$.

In summary, we have derived a simple expression involving a single integral that gives the complete scattering matrix for antiproton impact on atomic hydrogen. The theory is in remarkably good agreement with essentially exact calculations of ionization above 1 keV, and the KW or FMD calculations of protonium formation below 50 eV.

ACKNOWLEDGMENTS

This research has been supported by the Chemical Science, Geosciences and Biosciences Division, Office of Basic Energy Science, Office of Science, U.S. Department of Energy under Grant No. DE-FG02-02ER15283.

[1] E. A. Solov'ev, Zh. Eksp. Teor. Fiz. **70**, 872 (1976), [Sov. Phys. JETP **43**, 453 (1976)].
[2] D. R. Schultz, P. S. Krstić, C. O. Reinhold, and J. C. Wells, Phys. Rev. Lett. **76**, 2882 (1996).
[3] G. Schiwietz *et al.*, J. Phys. B **29**, 307 (1996).
[4] J. S. Cohen, Phys. Rev. A **56**, 3583 (1997).
[5] K. Sakimoto, Phys. Rev. A **65**, 012706 (2001); **66**, 032506 (2002); J. Phys. B **33**, 1349 (2000); **34**, 1769 (2001).
[6] K. A. Hall, J. F. Reading, and A. L. Ford, J. Phys. B **29**, 6123 (1996).
[7] A. Igarashi, S. Nakazaki, and A. Ohsaki, Phys. Rev. A **61**, 062712 (2000).
[8] B. D. Esry and H. R. Sadeghpour, Phys. Rev. A **67**, 012704 (2003).
[9] G. Ya. Korenman, J. Phys. B **13**, 641 (1980).
[10] J. S. Cohen, Phys. Rev. A **59**, 1160 (1999).
[11] J. S. Cohen, R. L. Martin, W. R. Wadt, Phys. Rev. A **24**, 33 (1981).
[12] C. L. Kirschbaum and L. Wilets, Phys. Rev. A **21**, 834 (1980).
[13] J. S. Cohen, Rep. Prog. Phys. **67**, 1769 (2004).
[14] Y. N. Demkov and V. I. Osherov, Zh. Eksp. Teor. Fiz. **53**, 1589 (1967) [Sov. Phys. JETP **26**, 916 (1968)]; see also Yu. N. Demkov and V. N. Ostrovskii, *Zero-Range Potentials and Their Applications in Atomic Physics* (Plenum, New York, 1988).
[15] L. V. Komarov, L. I. Ponomorav, and S. Yu. Slavyanev, *Coulomb Spheroidal Functions* (Nauka, Moscow, 1976), p. 320.
[16] S. Yu. Ovchinnikov and J. H. Macek, Phys. Rev. A **55**, 3605 (1997).
[17] D. I. Abramov, S. Yu. Ovchinnikov, and E. A. Solov'ev, Phys. Rev. A **42**, 6366 (1990).
[18] P. R. Žďánká, H. R. Sadeghpour, and N. Moiseyev, J. Phys. B **37**, L35 (2004).